Journal of Materials Processing Technology 223 (2015) 299–304

Contents lists available at ScienceDirect

Journal of Materials Processing Technology

journal homepage: www.elsevier.com/locate/jmatprotec

Constant current vs. constant power control in AC resistance spot welding

Zhou Kang[a,b,*], Yao Ping[c], Cai Lilong[b]

[a] State Key Laboratory of High-Temperature Gas Dynamics, Institute of Mechanics, Chinese Academy of Sciences, Beijing 100190, China
[b] Department of Mechanical and Aerospace Engineering, Hong Kong University of Science and Technology, Hong Kong, China
[c] College of Electromechanical Engineering, Guangdong Polytechnic Normal University, Guangzhou 510635, China

ARTICLE INFO

Article history:
Received 23 October 2014
Received in revised form 15 April 2015
Accepted 16 April 2015
Available online 24 April 2015

Keywords:
Control strategy
Constant current control
Constant power control
Nugget growth

ABSTRACT

Constant current control (CCC) and constant power control (CPC) are two of the most popular control strategies employed in resistance spot welding (RSW). They have their individual respective advantages; for example, with CCC, it is easy to control energy delivery, while CPC can deliver more heat in particular situations. CPC can be accomplished by means of CCC. The performance of CPC is not as good as that of CCC, because CPC involves more interfering elements. Dynamic resistance is employed to analyze the welding process. Corresponding analysis shows a more reliable welding process can be obtained and the first melting point can be detected earlier when CCC is employed rather than CPC. Though the overall nugget growth trends may show a very small difference when using one strategy versus the other, CCC can provide a larger nugget size because the initial energy allotment is more reasonable and the energy delivery is much steadier. We conducted experiments to validate all of the theoretical analysis. This work can serve to inform actual welding production to obtain a more reliable welding process, enable welders to choose a proper control strategy and help improve energy efficiency in practice.

1. Introduction

In single-phase AC resistance spot welding (RSW) machine operation, the power source utilizes two silicon-controlled rectifiers (SCRs) to regulate the amount of energy delivered into the welding system. During each control cycle, the welding control action is to set a specific firing angle. This firing angle is also considered as the trigger time and is based on the trigger frequency of each SCR. There is then a burst of pulsed current, which is typically 5–20 kA, passes the welding load. Hence, there is only one input during each control cycle. In reality, Podržaj et al. (2006) pointed out that different combinations of firing angles and welding transformer settings can result in different welding current waveforms, which can significantly affect the welding quality, as well as behaviors such as expulsion, even when the average values of the welding currents are the same. However, the integrated RSW system is nonlinear and varies over time; this is caused by the electrical system involved in the inductive loads. The shape of the current wave is non-sinusoid when the input voltage wave is a standard sine wave (Dhandapani et al., 1999). The welding load also varies over time during the welding process (Dickinson et al., 1980). In our previous work (Zhou and Cai, 2014a), the electrical structure was thoroughly analyzed and an appropriate constant current controller was developed, which considered the effect of time-varying and nonlinear characteristics in detail.

To establish a uniform nugget growth model and explore the physical characteristics of phase transition, an appropriate control strategy should be chosen so as to save welding energy and obtain welding products with satisfactory quality. However, during the welding process, the integrated dynamic resistance is the sum of resistances of liquid metal and solid metal, and the compositions of these metals are varying with time through the weld cycle. Controlling and analyzing target during the process is an integrated workpiece, rather than just liquid metal, which directly contributes to nugget growth. Nowadays, it is difficult to distinguish in real-time the composition of the nugget, because its variation is dynamic and hard to measure. Robert et al. (1996) analyzed the application of the finite element method in RSW, and pointed out the reason that the composition is difficult to determine was that the governing differential equation could not precisely predict heat transfer

* Corresponding author at: Chinese Academy of Sciences, Institute of Mechanics, No 15, Beisihuanxi Road, Haidian District, Beijing, China. Tel.: +86 10 82545985
E-mail addresses: zhoukang326@126.com, zhoukang@imech.ac.cn (K. Zhou), melcai@ust.hk (L. Cai).

http://dx.doi.org/10.1016/j.jmatprotec.2015.04.016
0924-0136/

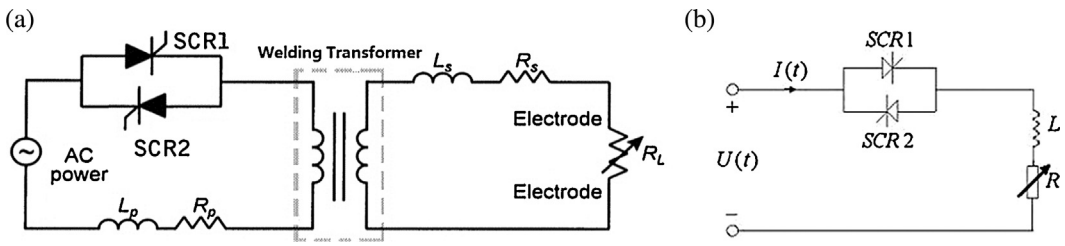

Fig. 1. (a). Electrical structure of an AC RSW; (b). Equivalent model of an AC RSW.

phenomena when phase changes were involved. Moreover, Podržaj et al. (2008) pointed out that corresponding sensors could not be properly mounted on the resistance spot welding system. Hence, designing an appropriate control strategy should be based on the mechanism of energy delivery and absorption, especially where the liquid nugget formation and growth are concerned.

Podržaj et al. (2008) illustrated three control strategies in detail: constant current control (CCC), constant voltage control (CVC) and constant power control (CPC), also called constant heat control (CHC). El-Banna et al. (2008) pointed out that CCC and CPC are the two most popular types of control strategies in practice. CCC only considers current variations, while CPC considers both current and electrode voltage variations. In practical application, the value of welding currents is always used as the control criterion, because this variable is easy to measure and can intuitively reflect the operation of energy input. On the other hand, the welding operation is a process of metal absorbing heat and then melting; hence, the amount of heat delivery is directly related to nugget formation and growth. In addition, Yu et al. (2014) concluded that the CPC strategy has an advantage of reducing expulsion at the early stage of the welding process; therefore, it may be able to deliver higher heat than that of CCC. Hence, both of these strategies have individual merits in practical application. To obtain more useful and constructive conclusions to instruct actual industrial production, the performance of these two strategies in actual application needs to be carefully considered.

In this paper, a comparison study between the CCC and CPC strategies is conducted. The effects and corresponding phenomena are collected and analyzed. The rest of this paper is organized as follows: Section 2 offers an explanation of the implementation of CCC and CPC; Section 3 provides a physical interpretation of the welding process and the effect of these two control strategies have on nugget formation and growth during the different stages of the welding process. The practical welding experiments and corresponding analysis are described in Section 4. Finally, Section 5 provides some concluding remarks for this work.

2. Realization of control strategies

The electrical system of an RSW machine comprises an AC power source, two reverse parallel SCRs, a welding transformer and welding loads. To conveniently and easily conduct corresponding analysis, the work of Baldwin et al. (2005) ignored the welding transformer and transferred all the components in the secondary coil to the primary coil. Fig. 1, which was discussed in our previous work (Zhou and Cai, 2014a), can show the electrical structure of an AC RSW and its equivalent model.

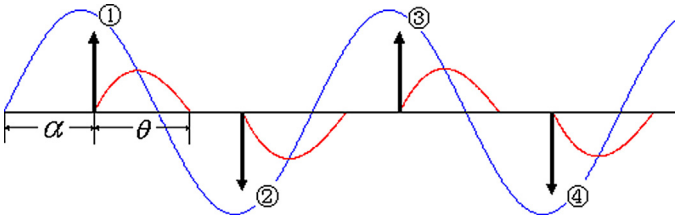

Fig. 2. Control cycle of a single-phase AC RSW machine.

In Fig. 1(a), L_p and R_p are the equivalent inductance and resistance in the primary coil of the welding transformer; while in the secondary coil, L_s and R_s denote the same corresponding parameters, and R_L is the welding workpiece, which lies between the upper and lower electrodes during the welding process. In Fig. 1(b), $U(t)$ is the mains voltage, and L and R denote respectively the equivalent inductance and resistance of the equivalent model.

Traditionally, in a single-phase AC RSW machine, the control frequency is twice the frequency of the AC power source, because two control actions can be conducted during one sinusoidal waveform of AC power. Fig. 2 shows 4 control cycles. In Fig. 2, α is the firing angle, and θ is the conduction angle, which denotes the actual effective period of the welding action. Hence, the control operation of RSW sets a proper firing angle α for each control cycle to determine how much energy is delivered into the welding system. One control cycle denoting one firing angle is set. The result of the energy delivery can be evaluated using the welding current or the energy absorbed by the workpiece, or other relative variables.

In our previous work (Zhou and Cai, 2014a), a CCC algorithm was developed. The algorithm is based on thoroughly analyzing the electrical system and establishing a model of the relationship between certain input variable, which is firing angle α, and a desired welding current. A proportional-derivative (PD) controller is employed to compensate for estimation error and improve performance. The mathematical description of the CCC controller can be written as follows:

$$\begin{cases} \tilde{\alpha}_{i+1} = \tilde{\alpha}_i + K_p(\hat{\alpha}_{i+1} - \tilde{\alpha}_i) + K_d[(\hat{\alpha}_{i+1} - \tilde{\alpha}_i) - (\hat{\alpha}_i - \tilde{\alpha}_{i-1})] \\ \hat{\alpha}_{i+1} = \dfrac{\arccos\left[\left(I_R^d/I_{R,i}^a\right) \times [\cos(0.1\pi\tilde{\alpha}_i) - \cos[0.1\pi(10+\psi_i)]\right] + \cos[0.1\pi(10+\psi_i)]]}{(0.1\pi)} \end{cases}, \quad (1)$$

where $\tilde{\alpha}$ is the actual firing angle of the controller; K_p and K_d are the feedback gains; $\hat{\alpha}$ is the estimation of the firing angle, which is obtained from the second equation in Eq. (1); I_R^d is the desired value of the welding current, I_R^a is the actual value of the welding current; i and $i+1$ denote the index of the control cycle; and ψ is the phase lag angle. The current value in this algorithm is the root-mean-square (RMS) value, which is commonly used in actual welding operations. In addition, in order to guarantee operational safety, Dennison et al. (1997) suggested that the first control cycle should use firing angle with a large constant value so as to deliver less energy into the welding cycle at the beginning of the welding operation.

According to Eq. (1), the corresponding CPC controller can be derived based on the relationship between energy and the welding current:

$$E = I^2Rt \tag{2}$$

where E is the amount of energy delivered, R is the dynamic resistance, and t is the duration of the number of seconds that pass as the current passes the welding load. Hence, the second equation in (1) can be written as:

$$\hat{\alpha}_{i+1} = \frac{\arccos[\sqrt{\left(E_R^d/E_{R,i}^a\right) \times \left(R^d/R_i^a\right)} \times [\cos(0.1\pi\tilde{\alpha}_i) - \cos[0.1\pi(10+\psi_i)]] + \cos[0.1\pi(10+\psi_i)]]}{(0.1\pi)}, \tag{3}$$

where in actual operation, the effect of the duration t can be neglected, because the ts in the various adjacent control cycles have only very small differences. However, the desired dynamic resistance cannot be directly obtained. Hence, we used the mean value of dynamic resistance during two adjacent control cycles as a substitute:

$$\hat{R}^d = \frac{R(i) + R(i-1)}{2}, \tag{4}$$

Correspondingly, the dynamic resistance of the ith control cycle can be replaced by the dynamic resistance of the $i-1$th control cycle. This not only makes the ratio of the two dynamic resistances reasonable, but also weakens the output fluctuation induced by actual imbalance between the positive trigger and negative trigger caused by the two SCRs having different voltage drops, which was illustrated in (Zhou and Cai, 2014c) in detail. Hence, the corresponding mapping between each firing angle and desired value of delivered power can be described as:

$$\hat{\alpha}_{i+1} = \frac{\arccos[\sqrt{\left(E_R^d/E_{R,i}^a\right) \times \left(\hat{R}^d/R_{i-1}^a\right)} \times [\cos(0.1\pi\tilde{\alpha}_i) - \cos[0.1\pi(10+\psi_i)]] + \cos[0.1\pi(10+\psi_i)]]}{(0.1\pi)}. \tag{5}$$

Combining Eqs. (4)–(5) with the PD controller in Eq. (1), a constant power controller can be developed. The controller is developed based on our previous constant current controller and has an approximate structure, which needs to be validated via an actual welding operation at a later time.

3. Physical interpretation of the process

Welding control is an energy-delivery controlling process, while the process of nugget formation and growth is determined by the metal absorbing energy and melting. The basic Joule heat generating formula can be employed to interpret the process:

$$Q = \int_{T_1}^{T_2} I(t)^2 R(t) \mathrm{d}t \tag{6}$$

where Q is the amount of heat generated in the weld, $I(t)$ is the welding current, $R(t)$ is the dynamic resistance of the sheet metals, and T_1 and T_2, respectively, denote the beginning and ending times of the operation.

Though dynamic resistance varies during the welding process, it does follow a certain rule. Dickinson et al. (1980) illustrated the variation rule of dynamic resistance. Our previous work (Zhou and Cai, 2014b) was also heavily focused on this rule. We used a figure to show the variation tendency of dynamic resistance in the work (Zhou and Cai, 2014b), and re-plotted it as shown in Fig. 3.

There are two particular points: one is the first melting point, and the other is the peak β. The first melting point is the beginning of nugget formation and growth. Before the first melting point, the dynamic resistance comprises pure solid metal resistance and the delivered energy does not contribute to nugget formation. Hence, the effective energy that contributes to nugget formation and growth should only be considered from this point, and the point can be detected in real-time using the first order derivative of the dynamic resistance curve, which is illustrated in our previous work (Zhou and Cai, 2013) in detail. During the welding process, the phase change can make the total dynamic resistance decrease due to the distance between the upper and lower electrodes being reduced, which causes the length of the current path to decrease. On the other hand, the rising temperature of the solid metal increases the total dynamic resistance as the resistivity of the solid metal increases with temperature. Hence, the peak β is the equilibrium between the increase and decrease of the total dynamic resistance.

According to the variations of dynamic resistance, CCC can be much more reliable than CPC. Using the CCC strategy, the current values are approximately similar in each control cycle, and the amount of energy delivered is proportional to the dynamic resistance variation, as shown in Fig. 3. It can be analyzed in detail using the amount of energy needed for the different welding stages. Before the peak β, the energy delivered is increasing, and a large amount of energy is needed because the energy should be used to eliminate surface contaminations and to contribute to initial nugget formation and growth. After β, the energy is decreasing according to the variation in resistance; the amount should be decreased gradually to allow the nugget size to achieve a predetermined goal in a short while. Hence, a smaller amount of delivered energy is more reliable, because the liquid nugget may approach the boundary between the workpiece and electrode, which could easily cause expulsion. In this situation, if CCC strategy is employed, the energy delivered is likely to be a correct amount. However, if CPC strategy is used, the amount of energy delivered is approximate, because the actual welding current is inversely proportional to the dynamic resistance, which is increasing before β and decreasing after β. Hence, the welding current is decreasing in the initial phase and increasing in the later phase; this is not efficient. Especially when the dynamic resistance experience a large decrease at the end of the welding process, the welding current may have a large increase, which may easily cause expulsion.

On the other hand, Yu et al. (2014) and Seo-Moon et al. (1997), according to theoretical analysis and experimentation, proposed that the CPC can reduce expulsion at the early stage of the welding process. Therefore, it is possible to deliver higher heat to the

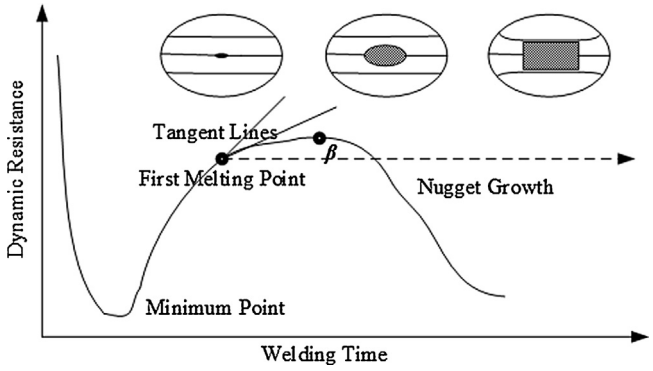

Fig. 3. Variation tendency of dynamic resistance.

welding system. In some instances, a larger nugget size or higher tensile shear strength can be obtained when CPC is employed than when CCC is used. Moreover, CPC can have a larger welding range in terms of total heat delivery, and it can show better weldability for coated steel and under different electrode force conditions. Although these conclusions were drawn from the Medium Frequency Direct Current (MFDC) RSW experiment, they also apply to single-phase AC RSW, for two reasons; (1) the working principles of these two types of RSW operations are similar, and (2) the dynamic resistance for the same workpiece has the same variation rule.

Additionally, while CPC guarantees constant energy delivery in each control cycle, the amount of energy is generated by the total workpiece, which includes solid metal and liquid metal; therefore, nugget growth may not be as steadily as expected. Any trigger time for the next control cycle in the CPC controller involves integrated dynamic resistance, as shown in Eq. (5). Hence, before the first melting point, the trigger time calculation may have a large fluctuation because dynamic resistance can change significantly; this may affect detection of the first melting point. On the other hand, CCC only considers the input current, the calculation of which does not contain the dynamic resistance. This means that the control performance of CCC may be better than that of CPC. Also, because the energy delivery of CCC is steadier than that of CPC and is proportional to the dynamic resistance variation, CCC strategy is much better to eliminate surface contamination than CPC. A steady energy delivery process is also better for energy absorption and for decreasing energy losses. Because all of the delivered energy is well distributed to the target workpiece, the first melting point can be detected sooner using CCC than when using CPC.

Moreover, after the first melting point, the energy delivery should be directly related to the nugget formation and growth (Zhou and Cai, 2013). In the initial nugget formation phase, all of the internal energy contributes to heat the solid metals and then melt them, very few energy can dissipate into the air because of the large amount of surrounding metals. Hence, the initial nugget growth can be faster than that in latter phase, as well as the initial energy efficiency is higher. When CCC is employed, because of the same reasons that first melting occurs earlier, it can have faster nugget growth and lower amount of energy losses in initial phase than that of CPC. Then after a short while, as the amount of surrounding metals reducing, some energy can dissipate into the air, which induces the nugget growth speed and energy efficiency would be reduced. During the nugget growth stage, the dynamic resistance has relatively smaller change, there is not a great amount of difference between CCC and CPC. Hence, the overall nugget growth trends obtained using CCC and CPC may have only a small difference, since workpieces with similar sizes may incur similar overall energy losses in the phase changing process. Therefore, for the same amount of effective delivered energy, CCC should have a larger initial nugget size than CPC, due to the initial energy allotment is much reasonable and energy losses are fewer by CCC in the initial nugget formation phase. According to these analyses, using CCC may provide a larger nugget size than CPC when the same amount of energy is delivered.

4. Experiments and analysis

Practical welding experiments were conducted to explore the different effects of employing these two controllers. We used a 63 kV A single-phase AC RSW machine. The electrode force was determined by a pressure differential of two air pressure gauges. In this work, the air pressure applied was 0.18 MPa, which corresponds to approximately 5000 N of electrode force. The electrode geometry used was a truncated cone with a 60° angle and a 5 mm face diameter. Low carbon bare steel (DS) was used in all experiments, the chemical composition of which is shown in Table 1 (Zhang et al., 2000). The size of the sheet is 10 mm in width, 200 mm in length and 2 mm in height.

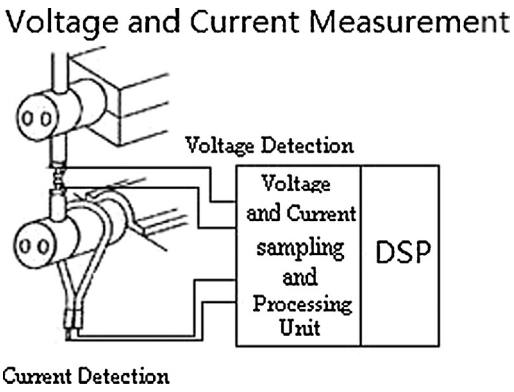

Fig. 4. Electrode voltage and welding current measurement device.

Both CCC and CPC experiments were conducted. The control actions were realized by a digital signal processor (DSP)-based control board. The DSP used dsPIC6014, which was manufactured by Microchip Technology Inc. All of the control algorithms and other relative operations were achieved using *C* language and then downloaded into the control board to execute. The electrode voltage was obtained by a tip voltage detection cable, while the welding current was detected by a Rogowski current transducer. The detailed measurements were the same as those taken in the previous work (Zhou and Cai, 2013), as shown in Fig. 4.

The originally collected data was processed using on-board hardware filters together with commonly used filter algorithms. For example, we used the mean value of each of the three data points to replace the original collected voltage and current data in order to conduct further processing. Then, the data was used to calculate the corresponding RMS values as follows:

$$\begin{cases} I_{\mathrm{RMS}} = \sqrt{\dfrac{1}{N}\displaystyle\sum_{i=0}^{N} i_d^2} \\ V_{\mathrm{RMS}} = \sqrt{\dfrac{1}{N}\displaystyle\sum_{i=0}^{N} v_d^2} \end{cases} \tag{7}$$

where i_d and v_d are, respectively, the original sampling welding current and electrode voltage data; and N is the number of sampling data obtained during each control cycle. The RMS values were calculated each control cycle. In this work, the frequency of data collection was 6.4 kHz, which means that 64 data points can be obtained during one control cycle if the conduction angle is 180°. In practice, it is impossible for SCR to be turned on all the time during one control cycle, and the conduction angle is always below 180°. For example, 90° conduction angle means that 32 data points can be obtained in one control cycle. The calculations of the RMS values of current and voltage were based on the collected data. Then the dynamic resistance for each control cycle was obtained using V_{RMS} and I_{RMS}:

$$R(j) = \frac{V_{\mathrm{RMS}}(j)}{I_{\mathrm{RMS}}(j)}. \tag{8}$$

Table 1
Chemical composition (wt. %) of the workpieces used in these experiments.

C	Mn	P	S	Si	Cu	Ni	Cr	Mo	Sn	Al	Ti
0.035	0.210	0.006	0.011	0.007	0.020	0.009	0.033	0.006	0.004	0.037	0.001

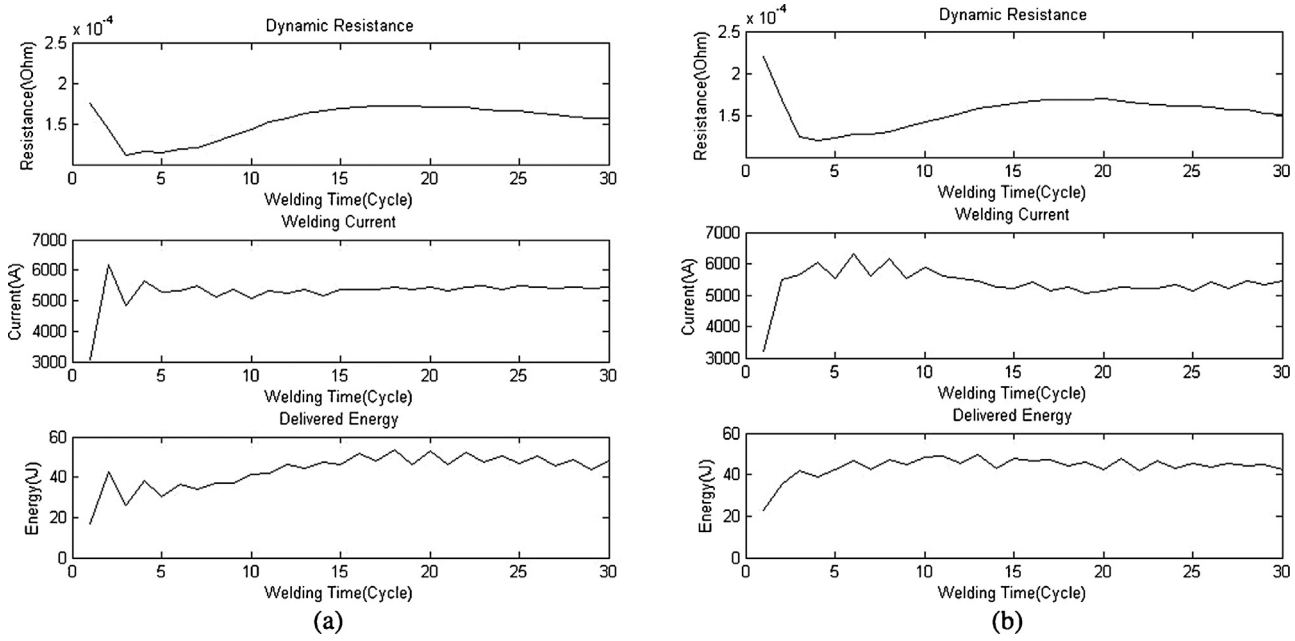

Fig. 5. (a). Experimental results using the CCC controller; (b). Experimental results using the CPC controller.

This equation can be used to calculate the dynamic resistance in the jth control cycle. The energy delivery in each control cycle, can be obtained according to the following equation:

$$E(j) = \sum_{i=1}^{N} U(i)I(i)t. \tag{9}$$

where j is the index of the control cycle, because the energy calculation is based on each control cycle; N denotes the number of sampling values within one control cycle; U and I are the actual values of electrode voltage and welding current and t is the data calculating cycle.

To obtain more reasonable comparison results, after several trials, we decided to use 5400A of welding current in CCC and 45 J of energy delivery in CPC, because we must approximate the corresponding energy and welding currents when working with the different controllers. To guarantee the safety of the operation, the trigger time for the first control cycle was 7.0 ms, corresponding to the 126° firing angle. Moreover, the parameters of the PD controller used the same values as were used in Zhou and Cai (2014a), which were $K_p = 0.55$ and $K_d = 0.3$. First, the effect of CCC and CPC may be examined. Fig. 5 shows the experimental result using CCC and CPC controllers, respectively.

The welding cycles were 30; in other words, 30 arrays of experimental data, including dynamic resistance and welding current and energy, were collected and are shown in Fig. 5. The dynamic resistance profiles were approximately the same. Both of the dynamic resistance curves followed the trend shown in Fig. 3. The control cycle when the first melting occurred can also be detected in real-time. The control performance of CCC and CPC can be checked numerically. To obtain a reliable comparison, only data after the first melting point was considered. The control cycles when the first melting occurred in these two experiment were the 9th cycle and the 10th cycle. For the CCC experiment, the largest error percentage was 1.49%, while the largest error percentage was 9.6% for the CPC experiment. It is obvious that the control performance of CCC was much better than that of CPC.

To explore the energy efficiency and nugget sizes obtained by these two control strategies, more experimental data should be employed. 12 arrays of CCC and 13 arrays of CPC experimental data were chosen. During the experiments, the control cycle when the first melting point occurred was recorded. The average value of the control cycle when the first melting point occurred using CCC was 8.25; this value was 9.15 when CPC was used. The results validate that the first melting point can occur earlier when CCC is used. Also, the nugget diameters, which can usually be used to describe the nugget size (Ouafi et al., 2010), were offline measured. Then, the relationship between the energy delivered after the first melting point and the nugget diameter can be obtained, as shown in Fig. 6. To observe the trend of the nugget growth, two straight lines were employed together with the scatter figures.

Because very small nugget diameters were difficult to be collected and accurately measured, and their data were not important for comparing the CCC and CPC, the nugget diameters in Fig. 6 began from the data which were easily collected. It can be observed that when the same amount of energy is absorbed by the workpieces, the nugget diameters obtained using CCC are larger than those obtained using CPC. Also, we can notice that the trends of nugget growth using these two different control strategies have little difference; as depicted in Fig. 6, the two scatter figures can be fitted approximately by two parallel straight lines in this certain range according to the experimental results, whose slopes were 0.0027923, though some measurement errors existed. It should be noticed that the straight lines cannot be considered as an actual mathematical relation between nugget diameter and energy. Actually, the accurate and integrated relation between them after the first melting point can be more elaborate instead of being described by a simple straight line curve fitting. This means that after the first

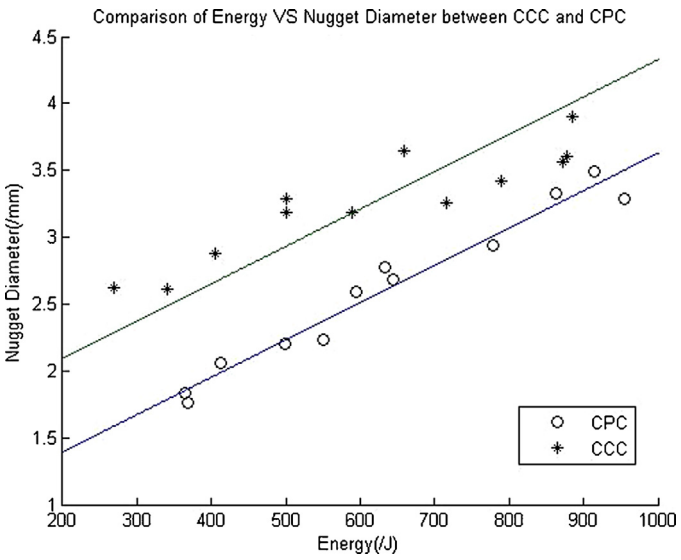

Fig. 6. Comparison of energy versus nugget diameter between CCC and CPC.

melting point, because the dynamic resistance had a steady variation, the energy delivery using CCC approximated that delivered using CPC. This also validates that the energy efficiency, which we may also call the net energy, for nugget growth after the first melting may be approximate, no matter which energy-delivery strategy was employed.

5. Conclusions

CCC and CPC are two popular control strategies employed in RSW operations. Their individual merits have been mentioned in much previous research. This work is conducted to further compare them. According to the theoretical analysis and experimental results obtained in this work, the following conclusions may be drawn:

1. CPC can be easily accomplished based on CCC; however, CPC cannot perform as well as CCC.
2. Theoretical analysis shows the welding process may be more reliable when CCC is employed, and the first melting may occur earlier, because the energy delivery is steadier and the initial energy allotment is more reasonable when CCC is employed.
3. CCC can obtain a larger nugget size than CPC for the same amount of energy delivery. This is because the initial nugget is larger; however, after the first melting point, the overall nugget growth trends obtained using the different two control strategies showed little difference for the same amount of energy delivery.

This work can serve for the welding industry to obtain a more reliable welding process, choose the most proper control strategy based on the characteristics of the workpieces, and improve the energy efficiency to save costs in practice.

Acknowledgements

The authors would like to thank the Research Grants Council of Hong Kong, China for financial support for this work (Project No: GRF 610611), and the characteristics of Guangdong Province ordinary university innovation project (2014KTSCX145).

References

Baldwin, T.L., Timothy Hogans, J., Henry, S.D., Frank Renovich, J., Latkovic, P.T., 2005. Reactive-power compensation for voltage control at resistance welders. IEEE Trans. Ind. Appl. 41, 1485–1492.
Dennison, A.V., Toncich, D.J., Masood, S., 1997. Control and process-based optimisation of spot-welding in manufacturing systems. Int. J. Adv. Manuf. Technol. 13, 256–263.
Dhandapani, S., Bridges, M., Kannatey-Asibu Jr., E., 1999. Nonlinear electrical modeling for the resistance spot welding process. In: Proceeding of American Control Conference, pp. 182–186.
Dickinson, D.W., Franklin, J.E., Stanya, A., 1980. Characterization of spot welding behavior by dynamic electrical parameter monitoring. Weld. J. 59 (Jun), 170s–176s.
El-Banna, M., Filev, D., Chinnam, R.B., 2008. Online qualitative nugget classification by using a linear vector quantization neural network for resistance spot welding. Int. J. Adv. Manuf. Technol. 36, 237–248.
Ouafi, A.E., Bélanger, R., Méthot, J.-F., 2010. An on-line ANN-based approach for quality estimation in resistance spot welding. Adv. Mater. Res. 112, 141–148.
Podržaj, P., Polajnar, I., Diaci, J., Kariz, Z., 2008. Overview of resistance spot welding control. Sci. Technol. Weld. Joining 13, 215–224.
Podržaj, P., Polajnar, I., Diaci, J., Kariz, Z., 2006. Influence of welding current shape on expulsion and weld strength of resistance spot welds. Sci. Technol Weld. Joining 11, 250–254.
Robert, W., Messler, J., Jou, M., 1996. Review of control systems for resistance spot welding: past and current practices and emerging trends. Sci. Technol. Weld. Joining 1, 1–9.
Seo-Moon, J., Kim, G.-S., Kim, J.-M., Won, C.-Y., 1997. Power control of resistance spot welding system with high dynamic performance, industrial electronics, control and instrumentation, 1997. In: IECON 97. 23rd International Conference on, pp. 845–849.
Yu, J., Choi, D., Rhee, S., 2014. Improvement of weldability of 1 GPa grade twin-induced plasticity steel. Weld. J. 93, 78s–84s.
Zhang, H., Hu, S.J., Senkara, J., Cheng, S., 2000. A statistical analysis of expulsion limits in resistance spot welding. J. Manuf. Sci. Eng. 122, 501–510.
Zhou, K., Cai, L., 2013. Online nugget diameter control system for resistance spot welding. Int. J. Adv. Manuf. Technol. 68, 2571–2588.
Zhou, K., Cai, L., 2014a. A nonlinear current control method for resistance spot welding. IEEE/ASME Trans. Mechatron. 19, 559–569.
Zhou, K., Cai, L., 2014b. On the development of nugget growth model for resistance spot welding. J. Appl. Phys. 115 (164901), 164901–164912.
Zhou, K., Cai, L., 2014c. Online measuring power factor in AC resistance spot welding. IEEE Trans. Ind. Electron. 61, 575–582.